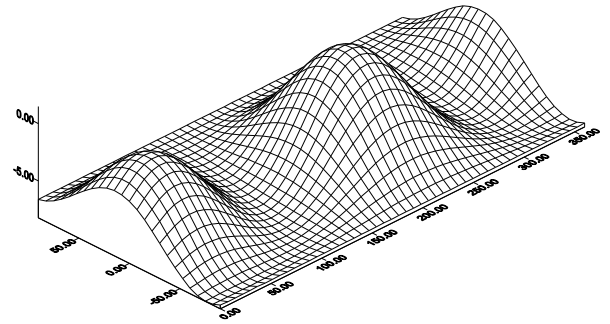
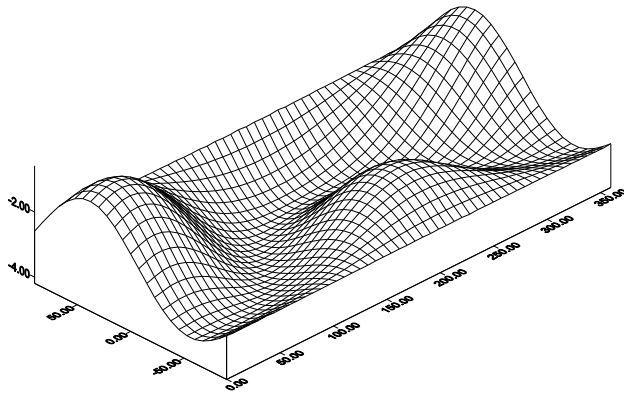


Fig.1 IMF modulus, SW velocity, SW temperature, SW density, time profiles of variations in global CR intensity with rigidity 4 (black line) and 20 GV (red line), changes of geomagnetic cutoff rigidity ΔR_c at

the point with threshold rigidity $R_c=4$ GV (red line) together with the Dst-index (black line), amplitudes of the first A_1 and second A_2 spherical harmonics of the CR pitch-angle anisotropy for particles with $R=4$ GV.

17h 29.10.2012

18h 29.10.2012



19h 29.10.2012

20h 29.10.2012

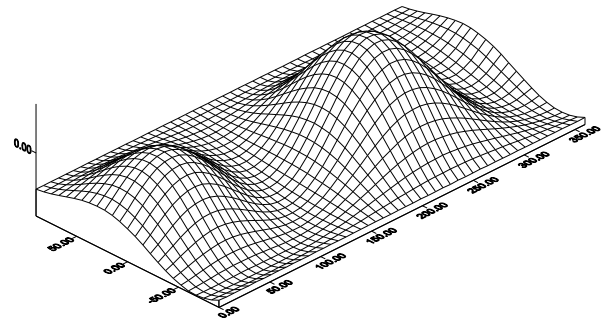
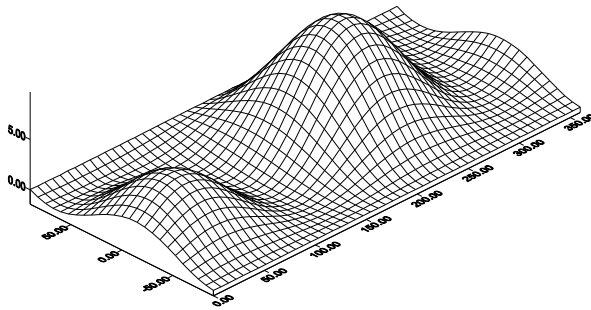


Fig.2 Relative changes in CR intensity with $R=4$ GV in the Geocentric Solar Ecliptic coordinate system for different time points on 29 October 2012.

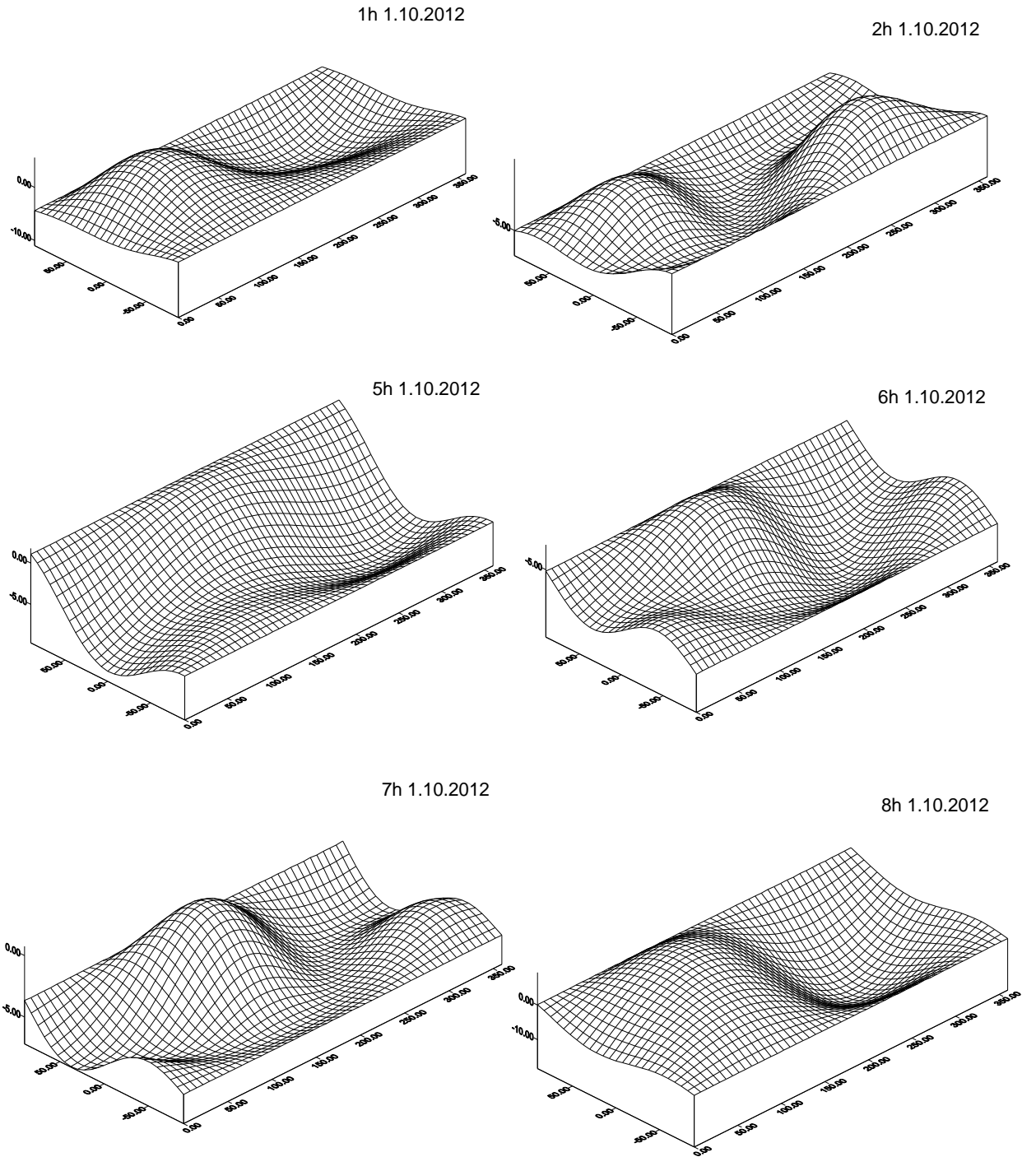
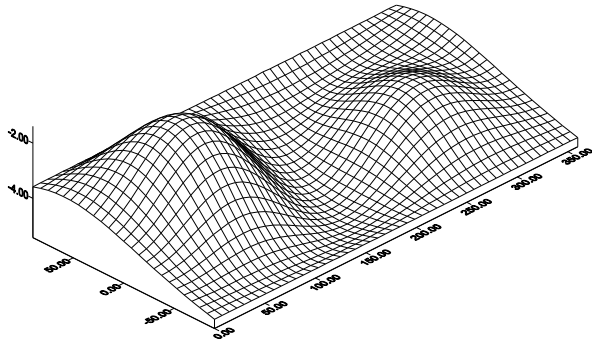
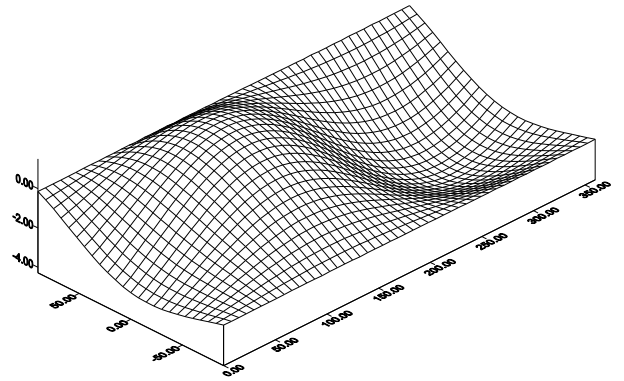


Fig.3 Relative changes in CR intensity c R=4 GV in the Geocentric Solar Ecliptic coordinate system for different time points on 1 October 2012.

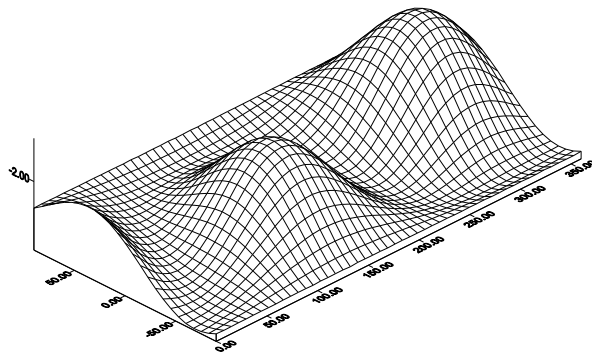
3h 8.10.2012



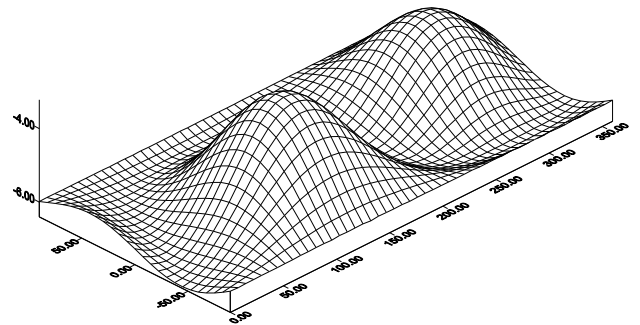
4h 8.10.2012



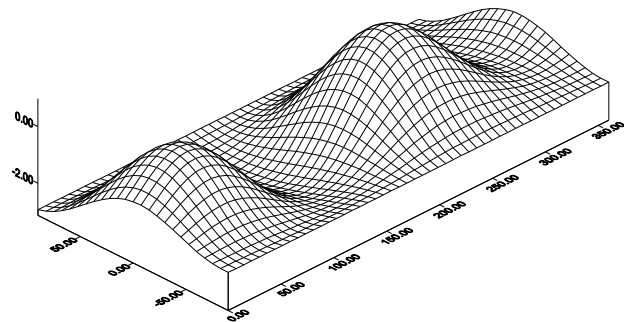
5h 8.10.2012



6h 8.10.2012



7h 8.10.2012



8h 8.10.2012

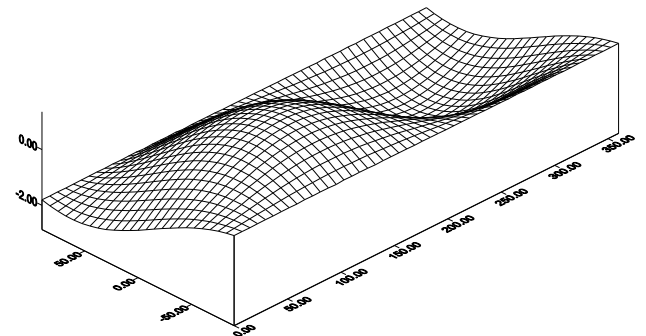


Fig.4 Relative changes in CR intensity c R=4 GV in the Geocentric Solar Ecliptic coordinate system for different time points on 8 October 2012.

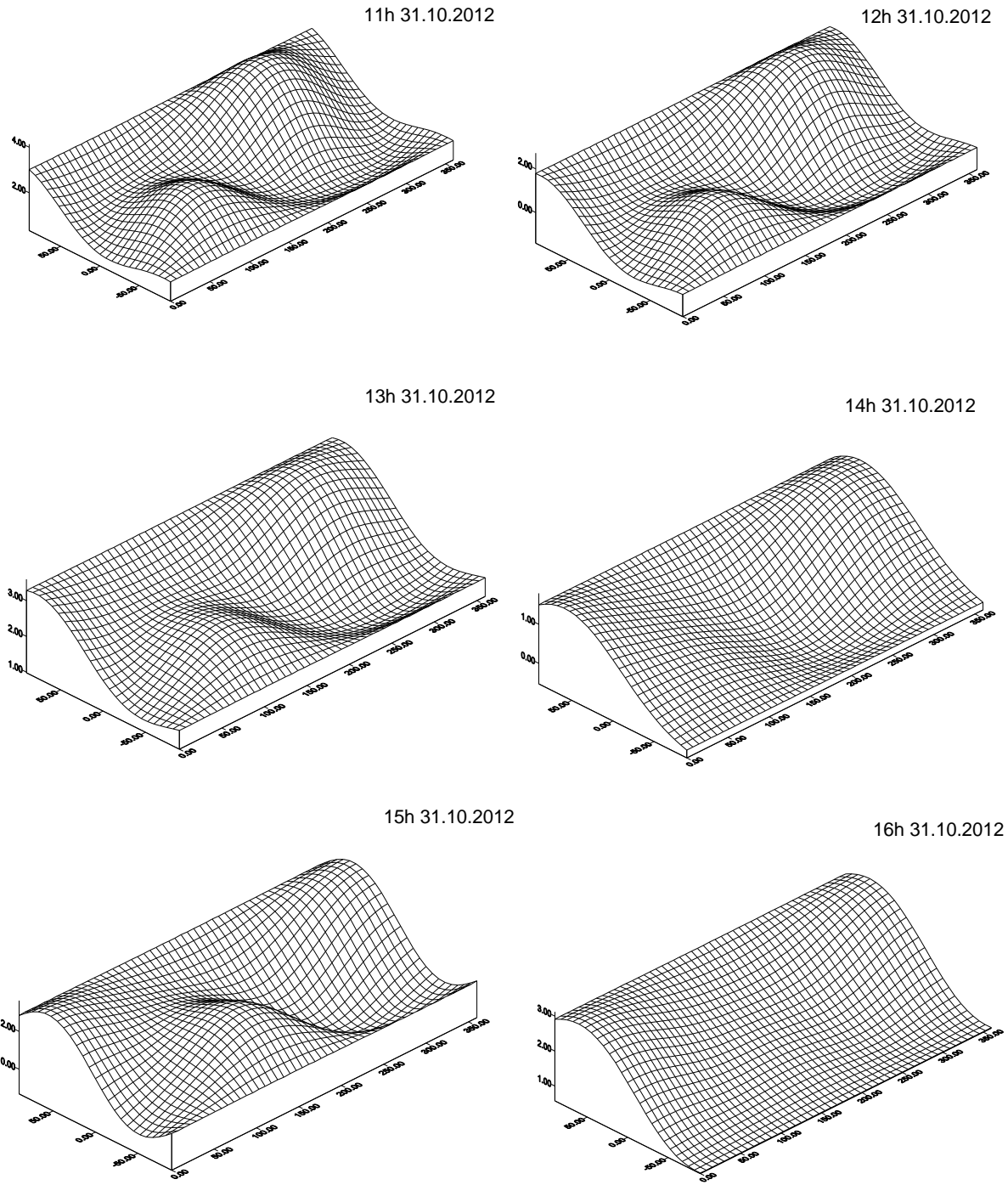


Fig.5 Relative changes in CR intensity $c R=4$ GV in the Geocentric Solar Ecliptic coordinate system for different time points on 31 October 2012.